A Cationic Stearamide-based Solid Lipid Nanoparticle for Delivering Yamanaka Factors: Evaluation of the Transfection Efficiency

Funda Alkan,[a] Hanife Sevgi Varlı,[a] Murat Demirbilek,[b] Engin Kaplan,[c] and Nelisa Türkoğlu Laçin*[a]

Induced pluripotent stem cells (IPSC) are preferred as an alternative source for regenerative medicine, disease modeling, and drug screening due to their unique properties. As seen from the previous studies in the literature, most of the vector systems to transfer reprogramming factors are viral-based and have some well-known limitations. This study aims to develop a non-viral vector system for the transfection of reprogramming factors. Cationic stearamide lipid nanoparticles (CSLN) were prepared via the solvent diffusion method. The obtained CSLNs were used for the delivery of plasmid DNA (pDNA) encoding Oct3/4, Sox2, Klf4, and GFP to fibroblast cell lines. The optimization studies, for zeta potential and particle size of the conjugate, was performed to achieve high cell viability. CSLN63 with 36.5 ± 0.06 mV zeta potential and 173.6 ± 13.91 nm size was used for the transfection of Fibroblast cells. The transfection efficiency was observed by following GFP expression and was found as $70\% \pm 0.11$. The expression of the Oct4, Sox2, Klf4 was determined by RT-qPCR; an increase was observed after the 12th cycle in Klf4 (Ct averages: 13,41), Sox2 (Ct averages; 12,4), Oct4 (Ct average; 13,77). The tendency of colonization was observed. The upregulation efficiency of Oct4 and SSEA-1 with CSLN and another non-viral vector designed for the transportation of Yamanaka factors developed in our lab previously were compared with flow cytometer analysis.

1. Introduction

The usage of stem cells for the treatment of various diseases is nowadays quite promising. The therapeutic use of stem cells obtained by reprogramming autologous somatic cells provides a significant advantage. Pluripotent stem cells can be isolated from the human embryo (embryonic stem cells) or can be obtained by reprogramming somatic cells (induced pluripotent stem cells). Induced pluripotent stem cells (IPSC) are new types of stem cells obtained by genetically reprogramming human or animal somatic cells. Induced pluripotent stem cells were first obtained in 2006 by reprogramming by the transfection of Oct4, Sox2, Klf4, and c-Myc genes via a viral-based carrier.[1] The IPSCs seem like a great solution for regenerative treatment by taking into consideration the immunologic rejection that can be faced with other cells and encountered ethical problems of embryonic cells.[2]

Viral and non-viral carriers are utilized as gene carriers for gene therapy for many years. The adeno-associated virus, retrovirus, adenovirus, and herpesvirus derived vectors are the most widely used viral vectors.[3] The main limitations of viral vectors for clinical applications are a possible immune response, the limited gene loading capacity, and the challenge of large-scale production.[4]

Additionally, one of the biggest concerns with the use of viral-based vectors is insertion mutagenesis resulting from the random integration of foreign viral DNA into the cell genome. Although some of the viral vectors remain episomally, they can still cause toxic effects and trigger the immune system.[5]

The transfection and gene expression efficiency of non-viral vectors compared to viral vectors are lower. However, they have various advantages in comparison to viral vectors such as ease of synthesis, production in large scale, high gene cargo capacity. Furthermore, non-viral vectors allow modifications for cell/tissue targeting due to chemical design flexibility[6,7]. Finally, non-viral vectors have low immunogenicity compared to the viral vectors. In recent years, non-viral vectors with high transfection efficiency similar to viral vectors have been produced thanks to the advances in nanotechnology.[8]

Generally, there are two main non-viral gene delivery vectors for nucleic acid. The polycationic polymers interact with the negatively charged DNA via electrostatic interactions. The cationic charge of a carrier vector allows passing through the negatively charged cell membrane easily.[9] Besides, cationic lipids have become increasingly popular against viral vectors nowadays. The immunogenicity of cationic lipids is low due to

[a] F. Alkan, H. S. Varlı, Ph.D. N. T. Laçin
    Yıldız Technical University
    Molecular Biology and Genetic Department
    Istanbul 34220
    E-mail: nelisalacin@gmail.com
[b] Ph.D. M. Demirbilek
    Hacettepe University, Advanced Technologies Application and Research Center Beytepe, Ankara 06800 (Turkey)
[c] Ph.D. E. Kaplan
    Bülent Ecevit University
    Faculty of Pharmacy
    Zonguldak (Turkey)

ChemistryOpen

Full Papers
doi.org/10.1002/open.202000244

Chemistry Europe
European Chemical
Societies Publishing

the polymeric vectors. Moreover, their similar chemical structure to cell membranes helps them to deliver their cargo to the cytoplasm quite easily.[10]

Besides, the solid lipid nanoparticles are composed of compounds that can be physiologically well tolerated, can be easily produced on a large scale, and have the potential of storage after freeze-drying.[11] They can be easily sterilized and demonstrate low cytotoxicity when injected intravenously.[12] The size of solid lipid nanoparticles is appropriate to travel through the microvascular system and has the ability to prevent macrophage uptake.[13] Targeting nanoparticles to intended tissues via size tuning, attaching a ligand to the surface of the nanoparticles, or using magnetic routing is also accomplishable.[14] The positively charged nanoparticles interact with negatively charged DNA through electrostatic interactions and form a conjugate.[15] Furthermore, particle aggregation is less likely to occur due to the electrical repulsion of a nanoparticle system with high zeta potential. The surface charge of nanoparticles is critical since it determines the interaction with the biological environment and the electrostatic interaction with the bioactive compounds.[16]

The solid lipid nanoparticles containing highly branched poly (β-amino ester)[17] and Zinc (II)-coordinative polyethyleneimine[18] is a significant examples of efficient and safe non-viral gene delivery system.

The zeta potential of nanoparticles is about the surface charge properties of the nanoparticle and is influenced by the composition of the environment. Since cellular membranes are negatively charged, the cationic nanoparticles tend to pass through the cell membrane.[19] The particle surface charge also plays a critical role in terms of targeting and clearance. In general, opsonins adsorb readily to negatively charged nanoparticle surfaces and lead to rapid removal from the blood circulation by reticuloendothelial system macrophages.[20]

Stearamide belonging to the class of organic compounds known as carboxyimidic acids, is a lipid already located in the cell membrane and cytoplasm. This study is the first in literature using stearamide as a lipid nanoparticle. Stearamide has been used in several studies, only to functionalize the nanoparticle surface.[21]

In this study, stearamide-based cationic nanoparticles were produced with a positive charge of 20 mV approximately, and the size of the nanoparticles was between 150–200 nm. Cationic stearamide-based nanoparticles were prepared using the solvent diffusion method. Cetylpyridinium chloride and cetyltrimethylammonium bromide were used as positive surfactants. The physicochemical properties of the obtained nanoparticles were examined by zeta sizer and a scanning electron microscopy (SEM). The (Solid lipid Nanoparticle) SLNP was used to transfer pDNA encoding the Oct3/4, Sox2, Klf4 genes to L929 fibroblast cells. Cell cytotoxicity of the SLNP system was determined on the mouse fibroblast-like cell line (L929). The octadecylamine-based lipid nanoparticle (OLN) was prepared in our previous studies,[22] and the two novel nanocarrier systems for cell reprogramming were compared in this study.

2. Materials and Methods

2.1. Materials

Stearamide (Octadecanamide, molecular weight (Mw) = 283.5), cetylpyridinium chloride (CPC), cetyltrimethylammonium bromide (CTAB) were supplied by from Merck (Germany). Fetal Bovine Serum (FBS), Trypsin-Ethylenediamine tetra acetic acid (Trypsin-EDTA), Dulbecco's Modified Eagle's Medium (DMEM) with glutamine and DMSO (Dimethyl sulfoxide) were purchased from Biological Industries (Israel). Dulbecco's modified Eagle's medium (DMEM/F12), 2-Mercaptoethanol, Minimum essential medium non-essential amino acids, basic fibroblast growth factor (bFGF) were purchased from Gibco, Life Technologies (Grand Island, NY). pDNA used for transfection of fibroblast cells Human 4-in-1 iPSC PiggyBac Vector (Cat. #PB210PA-1) (System Biosciences, USA).

2.2. Amplification and purification of pDNA

pDNA encoding the Oct3/4, Sox2, Klf4, and GFP was amplified in *E. coli* strain JM109. The purification process consisting of alkaline lysis, adsorption, washing, desorption steps were performed using the Qiagen Miniprep kit (Qiagen, USA). The obtained DNA was examined on a 1% agarose gel for 30 mins. Optical densities at the wavelength of 260 and 280 nm were determined with the Multiskan GO Microplate Spectrophotometer to determine the purity and concentration of pDNA.

2.3. Solid lipid nanoparticle synthesis

Two different nanoparticle systems were used in the study. The first one is the stearamide nanoparticle (CSLN), which was designed and synthesized in the study. The second system is octadecylamine nanoparticle (OLN), which has been synthesized in our previous studies.[22]

The stearamide nanoparticle was synthesized by the solvent diffusion method, and parameters were optimized to obtain convenient particle size and zeta potential. Briefly, 0.75 M stearamide was dissolved in 4 mL of chloroform-ethanol (1:1) solvent system to obtain a stearamide solution as a lipid phase. Various surfactants of different concentrations were studied for the preparation of positively charged nanoparticles in the 150–200 nm range. Mostly, the surfactant phase is prepared by one of Tween 80, Tween 40, sodium dodecylbenzene sulfonate (SDBS), cetyltrimethylammonium bromide (CTAB), and cetylpyridinium chloride (CPC). Among these surfactants, SDS and SDBS are anionic surfactants, Tween 80 and Tween 40 are non-ionic surfactants, while CTAB and CPC are cationic surfactants. The effect of these surfactants on the nanoparticle charge was examined, and a positive charge was tried to be obtained. The lipid phase added dropwise to the surfactant phase on a magnetic stirrer at 1500 rpm. After the dropping process, a single emulsion was prepared by homogenizing the lipid solution to the surfactant phase by the sonic probe (30%

ChemistryOpen

Full Papers
doi.org/10.1002/open.202000244

Chemistry Europe
European Chemical
Societies Publishing

amplitude, 50 sec). The nanoparticle solution was held on the magnetic stirrer at 800 rpm for 4–5 hours to remove chloroform and ethanol from the nanoparticle solution. The obtained stearamide nanoparticles were precipitated by centrifugation at 12,000 rpm for 30 min, followed by washing with distilled water several times and then lyophilized for storage.

2.4. Characterization of CSLN Nanoparticles

Scanning electron microscope (Zeiss, EVO® LS 10) has been used for the characterization studies of nanoparticles to determine particle size distributions and surface morphological properties. The nanoparticles obtained in solid form are characterized. The mean size-size distribution, surface charge, and polydispersity index (PDI) value of the stearamide based nanoparticles were determined by Zeta Sizer (Malvern Nano ZS, UK) with three replicates (n:3). The characterization of OLN nanoparticles was performed in our previous studies.[22]

2.5. In-vitro cytotoxicity of CSLN Nanoparticles

MTT assay was performed to determine the in vitro cytotoxicity of CSLN on L929 fibroblast cells. 10^4 cells/well were seeded in 96-well plate. L929 cells were cultured in DMEM medium containing 10% FBS, 1% L-glutamine; cultured at 37°C with 5% CO_2 atmosphere for 24 hours. CSLN was added to each well at different concentrations as 10.3, 20.6, 25.75, 30.9, and 41.2 μg/well on a 96-well plate and incubated for 24 hours. Then, the medium was removed, and each well was treated with 3-(4 5-dimethylthiazol-2-yl)-2 5-diphenyltetrazolium bromide (MTT) (5 mg/mL in medium) and incubated for 4 h at 37°C with 5% CO_2. Then, the MTT solution was removed, and 100 μL DMSO was added to each well to dissolve the formazan crystals. The optical density was determined at 570 nm by Elisa reader (Thermo Scientific Multiskan Go, USA). MTT analysis was performed in eight replicates (n:8)

2.6. Transfection L929 cells by CSLN/pDNA and OLN/pDNA conjugates

Serum-free DMEM medium, DMEM medium containing 10% FBS and were used for transfection in the L929 cell line. Cells were seeded in 6 well plates 24 hours prior to transfection at a density of 8×10^4 cell/well and incubated overnight. One hour before transfection, medium replaced with a serum-free and antibiotic-free medium. pDNA/lipid-based vector conjugations were prepared by introducing the pDNA with NPs in PBS solution. The ratio of CSLN-pDNA and OLN-pDNA were both as 40 μL(1μg/μL) nanoparticle: 8 μL of pDNA (2 μg/μL). The size and zeta potentials of CSLN/pDNA conjugates were determined by Zeta Sizer (Malvern NanoZS, UK) with three replicates (n:3). The results were given in Table 2. The conjugate solutions were added to wells after incubation at room temperature for 15–20 minutes to maintain electrostatic interaction. Transfected

cells were incubated in a carbon dioxide incubator 4 hours. Then, the medium containing nanoparticles was replaced with DMEM medium containing 10% FBS. The plate was incubated at 37°C with 5% CO2 incubation for 24 h.

2.7. Evaluation of transfection efficiency of cationic lipid-based nanoparticle-pDNA conjugates

Transfection efficiency was assessed by visualizing the expression of GFP (green fluorescent protein) proteins by fluorescence microscopy for 72 hours. Besides, the transcription efficiency of genes was established by the RT-qPCR method. RNA isolation was performed from cells transfected using the GeneJET RNA purification kit (Thermo Scientific). cDNA was obtained from 1 μL RNA using the First Strand cDNA synthesis kit (Thermo Scientific). Oct3/4, Sox2, Klf4, and gene regions of the cDNA samples were targeted with the primers used by Eun Young et al.[23] RT-qPCR was performed with the AriaMax Real-Time PCR System (Agilent Technologies, USA) using SYBR Green-based Glossy III Ultra-Fast RT-qPCR Master Mix. The GAPDH mRNA region was targeted as a positive control in the reaction. The RT-qPCR analysis was performed in two replicates for each gene ($n = 2$).

2.8. Evaluation of transfection efficiency

Flow cytometry was performed for a precise evaluation of transfection efficiency, using the following primary and secondary antibodies: Anti-Oct4 antibody (Abcam, ab19857), Goat Anti-Rabbit IgG H&L (Alexa Fluor® 488, Abcam, ab150077), Anti-SSEA4 antibody (MC813, Abcam, ab16287), Goat Anti-Mouse IgG H&L (Alexa Fluor® 568, Abcam, ab175473). Cells were transfected with the naked pDNA, OLN-pDNA conjugate, and CSLN-pDNA conjugate. Cells were dissociated from the cell culture flask using TPP cell scraper (Product No. 99002, TPP Techno Plastic Products AG, Switzerland) on the third day. Then centrifugated at 2100 rpm for 5 min and resuspended in 100 μL ice-cold PBS, 10% FBS, 1% sodium azide. Primer and seconder antibodies dilutions were prepared as 3% BSA/PBS. The cells were incubated for 30 minutes with primary antibodies in 3% BSA/PBS solution at room temperature. The cells were washed 3 times by centrifugation at 2100 rpm for 5 min and resuspended in ice-cold PBS. The fluorochrome-labeled secondary antibodies in 3% BSA/PBS were added, and cells were incubated for 30 minutes at 4°C in the dark. The cells were washed three times by centrifugation at 2100 rpm for 5 min and resuspended in ice-cold PBS, 3% BSA, 1% sodium azide. The cell suspension was kept at 4°C in the dark. The analysis was performed with three replicates (n:3) on the NovoCyte Flow Cytometer System in the flow cytometry facility at Istanbul University Aziz Sancar Institute of Experimental Medicine.

ChemistryOpen

Full Papers
doi.org/10.1002/open.202000244

Chemistry Europe
European Chemical
Societies Publishing

2.9. Differentiation of reprogrammed fibroblast cells into IPS cells

Pluripotent stem cells must be maintained in special conditions to avoid differentiation. Matrigel, which is a mixture of proteins used as a basement membrane matrix for stem cells, is gelatinous in structure and maintains stem cells at an undifferentiated state. For IPSCs, DMEM-F12 (Dulbecco's modified Eagle's) medium containing 10 ng/mL basic fibroblast growth factor (bFGF), 0.1 mM non-essential amino acids and 100 mM b-mercaptoethanol, 10% knockout serum and 1X GlutaMax were used.[24] Matrigel was melted on ice for 2 hours before usage and then poured 500 µL/well to a 24-well plate. Then, incubated for 10 mins at 37 °C. Following transfection, cells were harvested from plates by trypsinization and centrifuged at 765 g for 5 mins. The cell pellet was resuspended with 1 mL IPS medium and was slowly seeded onto Matrigel. The medium was refreshed every two days. The morphological changes of the cells on the matrigel were followed by an inverted microscope for 15 days.

2.10. Statical Analysis

Cell culture tests were performed in six to eight replicates. Microsoft Excel 16.16.6 was used in the studies. Complementary statistical studies of the results and later variance analysis was made. Comparisons, according to the F account and F table values obtained after the variance analysis, were made using t-test equal or different variance. P-value < 0.05 was considered.

3. Results

3.1. Amplification and purification of pDNA

pDNA encoding Oct 3/4, Sox2, Klf4 was amplified and purified. DNA quantification was performed by a micro Drop plate (Thermo Scientific, USA). The purity (260/280 nm) of the isolated pDNA were 1.7 and 1.8. The concentrations of isolated pDNAs are (1.02 µg/µl) and (1.04 µg/µl), respectively. The agarose gel images of the pDNA is given in Figure 1.

3.2. Characterization of nanoparticle

Surface morphology analysis of cationic stearamide nanoparticles was performed with a Scanning Electron Microscopy (SEM Zeiss, EVO® LS 10) and shown in Figure 2. Zeta potential and particle size determinations were carried by a Zeta-Sizer. The nanoparticle charge and size varied depending on the type and amount of surfactant used, as seen in Table 1. SEM images revealed that the nanoparticles with a size of 173.6 ± 13.91 nm with a spherical structure were obtained with an almost narrow size distribution, as seen in Figure 2. The polydispersity index of the particles was 0.257 ± 0.05.
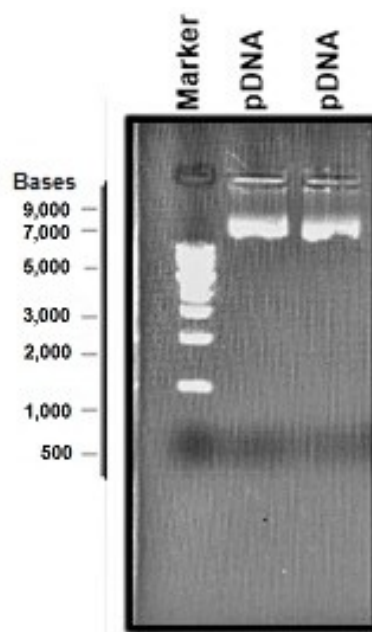

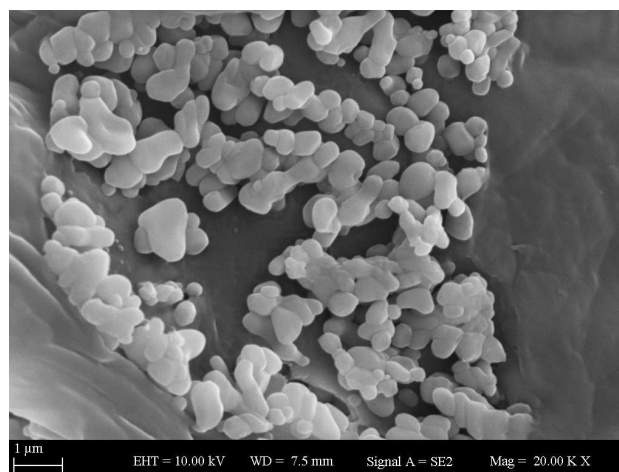**Figure 1.** Agarose gel image of pDNA.

Figure 2. Scanning electron micrograph of CSLN nanoparticles.

The size of the CSLN I nanoparticle synthesized using Tween 80 was determined as 826.5 ± 18.44 nm. The size of the CSLN II nanoparticle synthesized using Tween 40 was determined as 760.1 ± 30.42 nm. CSLN III nanoparticle prepared using SDBS; the size was reduced; however, the surface charge was found negative. CPC (cetylpyridinium chloride) was used as a positive surfactant to increase the surface charge. Since lipids tend to be aggregated according to their structure, the particle solution was held for 4–5 hours on the magnetic stirrer. As seen in the CSLN IV nanoparticle, the nanoparticle size was determined to be 216.2 ± 2.72 nm, and the zeta potential was $+16.02 \pm 2.50$ mV when CTAB (cetyl trimethyl ammonium bromide) was used as a cationic surfactant. The zeta potential of CSLN V has been determined as 46.7 ± 8.21 mV. Since the high positive charge has toxic effects on the cells,[25] the surface

ChemistryOpen

Full Papers
doi.org/10.1002/open.202000244

Chemistry
Europe
European Chemical
Societies Publishing

Table 1. ζ-average diameter and zeta-potential of the CSLN nanoparticles.

Formulation	Composition		Particle size/nm (S.D)	Polydispersity (S.D)	Zeta potential/mV (S.D)
CSLN I	Stearamide	0.125%	826.5 ± 18.44	3.78 ± 0.10	2.77 ± 3.29
	Tween 80	3%			
CSLN II	Stearamide	0.125%	760.1 ± 30.42	0.44 ± 0.20	5.16 ± 4.06
	Tween 40	3%			
CSLN III	Stearamide	0.125%	557.6 ± 25,04	0.376 ± 0.09	28.1 ± 5.3
	SDBS	1%			
CSLN IV	Stearamide	0.09%	216.2 ± 2.72	0.25 ± 0,11	16.02 ± 2.50
	CPC	0.03%			
	Tween 40	4%			
CSLN V	Stearamide	0.06%	217.8 ± 5.68	0.353 ± 0.02	46.7 ± 8.21
	CPC	0.06%			
	CTAB	0.3%			
CSLN VI	Stearamide	0.08%	173.6 ± 13.91	0.257 ± 0.05	36.5 ± 0.06
	CPC	0.04%			
	CTAB	0.2%			

Table 2. Zeta potentials and particle size of CSLN/pDNA conjugates.

CSLN-DNA Conjugate	CSLN	pDNA	Particle size/nm (S.D)	Polydispersity index (S.D)	Zeta potential/mV (S.D)
Conjugate I	32 μg (CSLN IV)	1 μg pDNA	461.1 ± 35.30	0.34 ± 0.04	−23.1 ± 5.3
Conjugate II	30 μg (CSLN VI)	1 μg pDNA	270.0 ± 35.1	0.4 ± 0.05	25.0 ± 1.75
Conjugate III	40 μg (CSLN VI)	2 μg pDNA	713.8 ± 10.4	0.42 ± 0.02	14.9 ± 0.361

charge of CSLN V was reduced by optimizing the ratio of stearamide and surfactant ratio. In this study, CSLN VI nanoparticles with 173.6 ± 13.91 nm size and 36.5 ± 0.06 mV charge preferred for the transfection to protect the fibroblast cells from the toxic effects of an excess hefty positive charge.

We synthesized stearamide-based cationic solid lipid nanoparticles for the first time as a non-viral vector. Stearamide-based lipid nanoparticles are rarely encountered in literature. In a study, nanoparticles from different lipid derivatives were synthesized to evaluate their anticancer activity on human colorectal cancer (CRC) cell lines. Stearamide derived particles were not spherical shape, and the particle sizes were 2273.67 ± 218.75 nm.[26] Ru et al. synthesized stearamide-based, cationic nanoliposomes and used for an antibacterial purpose.[21a] González-Paredes et al. modified the surfaces of anionic lipid nanoparticles by coating with cationic materials to enhance the delivery efficiency of the DNA.[27] Tabatt et al. used two different matrix lipids and six other cationic detergents obtain nanoparticles for DNA delivery. The particle size, zeta potential, DNA binding capacity, transfection efficiency, and cytotoxicity of lipid-derived nanoparticles were investigated. In the nanoparticle formulations using CTAB and CPC, the particle sizes were between 130 to 150 nm, and the zeta potentials of the particles were in the range of 35–45 mV. However, these formulations have been shown to have a toxic effect on the cells.[28]

3.3. In-vitro cytotoxicity of CSLN

The cytotoxicity of the cationic nanoparticle on the cell viability must be clearly defined. As it is well known, the toxic effect of lipid-based vector systems on the cell increases due to the amine groups in the structure. It was also stated that cytotoxicity increases as the positive charge increases.[29] In this study, the cytotoxicity of CSLNs on L929 was determined by the MTT test.[30] The related results were given in Figure 3.

SLN systems are highly effective and non-toxic DNA delivery systems for in vitro studies[31] The cell viability of CSLN-10,
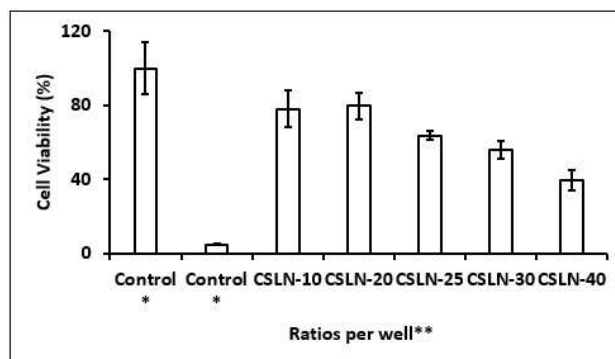

Figure 3. Cytotoxicity of cationic nanoparticles (*) DMEM was used as negative control, 1% DMSO was used as positive control (**) CSLN-10, CSLN-20, CSLN-25, CSLN-30 and CSLN-40 concentrations (n:8) were 10, 20, 25, 30 and 40 μL (1.03 μg/μL), respectively.

ChemistryOpen

Full Papers
doi.org/10.1002/open.202000244

Chemistry Europe
European Chemical
Societies Publishing

CSLN-20, CSLN-25, CSLN-30 and CSLN-40 was determined as 78%±9,90, 79%±6,97, 63%±2,37, 55%±4,76 and 39%± 5,25, respectively. According to these results, a high positive charge due to the increased ratio of nanoparticles showed a toxic effect against the cell. However, after the nanoparticle interaction with negatively charged DNA, the conjugate obtained will not present toxicity, since the positive charge of the conjugate will be significantly lower compared to the naked nanoparticle.

Choi et al., cationic lipid nanoparticles for the delivery of the P53 gene to lung cancer cells were synthesized. They have reported that particles as 69 nm and 8 mV, besides, had cytotoxicity below 20% on H1299 cells.[32] Kim et al. reported that the cationic lipid nanoparticles they prepared for gene silencing to deliver siRNA to the cancer cells had toxic effects with the increasing concentrations..[33]

3.4. Size and Zeta Potential of pDNA/CSLN Nanoparticle Conjugate

The nanoparticles must be cationic to form an electrostatic interaction with the DNA. It is also necessary to have an excess positive charge for the nanoparticle-pDNA conjugates to pass through the negatively charged cell wall.[34] Zeta-Sizer measurements of the nanoparticle/pDNA conjugates are given in Table 2. The size and potential of a conjugate vary depending on the zeta potential and size of the nanoparticle.[35] As shown in Table 2, the CSLN IV nanoparticle was interacted with pDNA, and the zeta potential of the conjugate was determined as −23.1±5.3 mV. The CSLN VI nanoparticle/pDNA (30:1) conjugate was selected with zeta potential 25.0±1.75 mV. The zeta potential of the CSLN VI nanoparticle/pDNA (40:1) conjugate was determined as 14.9±0.361 mV and preferred for transfection experiments to reduce the cell cytotoxicity that is induced by a positive charge.

3.5. Determination of Transfection Efficiency

L929 fibroblast cells were transfected with CSLN /pDNA conjugate (encoding GFP, Oct4, Klf4, and Sox2). For microscopic validation of transfection efficiency, transfected cells were monitored by a fluorescence microscope. Figure 4a-b shows the images of transfected L929 Fibroblast cells 24 hours later. Data shows that CSLN nanoparticles with 173.6 nm sized effectively transfer the pDNA to L929 fibroblast cells in vitro.

Lee et al. have developed new gene delivery systems using different cationic lipids for the treatment of cystic fibrosis. The transfection efficiency of these nanoparticles on the human bronchial epithelial cell line (CFT1) was determined in vitro. It has been reported that the transfection efficiency of the particles was between 50% to 70%.[36] Yu et al. evaluated the efficiency of an SLN for the delivery of siRNA. They reported that the anticancer effect was increased in accordance with the delivery of SLN. In this study, transfection efficiency was determined by imaging fluorescent protein expression. At the
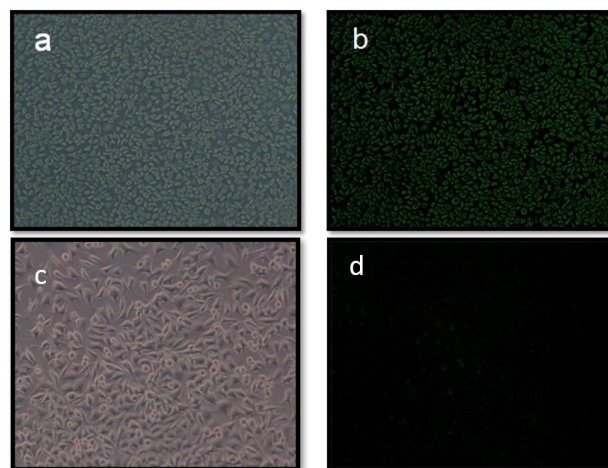

Figure 4. (a) 5x phase contrast images of transfected L929 Fibroblast cells with CSLN; (b) 5x fluorescence images of transfected L929 Fibroblast cells with CSLN; (c) 10× phase contrast images of transfected L929 Fibroblast cells with naked pDNA and (d) 10× fluorescence microscope images of transfected L929 Fibroblast cells with naked pDNA.

end of 24 hours, the density of transfected cells was reported to be between 60% and 70%.[37]

Klf4 (Kruppel-like factor 4), Oct4(octamer-binding transcription factor), Sox2 (SRY-Box Transcription Factor 2) are the essential transcription factors for the reprogramming of a somatic cell to a pluripotent stem cell. Thus, the Klf4, Oct4, Sox2, gene expression efficiencies in fibroblast L929 cells were determined.

Klf4, Oct4, Sox2 gene regions were amplified using specific primer pairs by real-time PCR. Amplification curves were given in Figure 5. The binary repeats of the gene regions are shown in the same colors. The line indicated by blue is the threshold value line. An increase was observed after 12th cycle in Klf4 (Ct averages: 13,41), Sox2 (Ct averages; 12,4), Oct4 (Ct average; 13,77). The amplification curves given in Figure 5 reveal that the mRNA levels of reprogramming factors Klf4, Oct4, and Sox2 in transfected and modified cells were significantly high compared to the native cell (non-transfected).
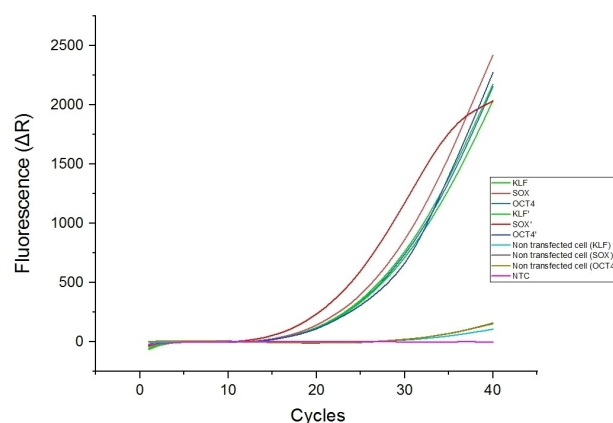

Figure 5. Amplification graph of reprogramming factors.

ChemistryOpen

Full Papers
doi.org/10.1002/open.202000244

Chemistry Europe
European Chemical
Societies Publishing

3.6. Flow Cytometry

On the third day of transfection, L929 fibroblast cells were harvested and analyzed by determining specific OCT-4 and SSEA-4 stem cells antibodies. The results were presented in Figure 6. Cells were determined by forward and side scatters and stained with SSEA4 and OCT4 to identify the pluripotency level and stemness of the transfected cells. Distinct populations were selected by removing dead cells. The levels of pluripotency markers OCT-4 and SSEA-4 have been detected for OLN-pDNA, CSLN-pDNA, and naked pDNA transfected cells.

The determinants OCT-4 and SSEA-4 expression in cells transfected with OLN-pDNA transfected cells were determined as $48.73 \pm 1.70\%$, as presented in Figure 6A. The determinants OCT-4 and SSEA-4 expression in cells transfected with CSLN-pDNA were determined as $39.43 \pm 0.05\%$ (Figure 6B). The determinants OCT-4 and SSEA-4 expression in cells treated with naked pDNA (Figure 6C) have shown significantly low expression as 2.64%.

Qu et al.[38] delivered transcription factors OCT4, SOX2, KLF4, and C-MYC (OSKM) to cells using a polycistronic plasmid to obtain iPSCs from adult human adipose-derived stem cells. Four days after double transfection, flow cytometry analysis showed that one-tenth of GFP positive cells. As a result of immuno-fluorescence staining of pluripotent markers and quantitative PCR analysis, reprogramming efficiency was found to be $0.006 \pm 0.0005\%$. Khan et al.[39] have developed a 1,12-diamino-dodecane-based non-viral vector for the generation of induced pluripotent stem cells. Reprogramming factors (recombinant proteins for Sox2, Nanog, Klf4, and NR5A) were delivered to fibroblast cells with these cationic bolaamphiphile carriers, and similar characteristics of the reprogrammed cells with embryonic stem cells were evaluated. Characterization of IPSCs by flow cytometry with antibodies against OCT3/4, Nanog, and SSEA4 revealed that approximately 80% of the cells were positive for these antibodies.

3.7. The Morphological Differentiation of Reprogrammed Cells

Morphological changes of transfected cells on the matrigel were observed with an inverted microscope for 12 days. The tendency of colonization in the cells was observed on the 7th day following the transport on matrigel. Images of transfected cells on matrigel are shown in Figure 7.

4. Conclusion

We aimed to develop a non-viral vector system for the transfection of Yamanaka factors efficiently. The size and charge of the solid lipid nanoparticles were found to be 173.6 ± 13.91 nm and 36.5 ± 0.06 mV. The SLN is considered suitable for gene transfer based on their size and zeta potential. SLN/pDNA (Klf4, Sox2, Oct4, and GFP) conjugate was used for the transfection of L929 fibroblast cells. The GFP expression efficiency was found as $70\% \pm 0.11$. According to the data obtained from RT-qPCR, the transfection factors Oct4, Sox2, and Klf4 were increased significantly starting from day 4. The tendency of colonization was observed with the transfected cells. As a result of the characterization of IPSCs by flow cytometry, the expression of OCT-4 and SSEA-4 in cells transfected with OLN-pDNA was $48.73 \pm 1.70\%$, while it was $39.43 \pm 0.05\%$ in cells transfected with CSLN-pDNA. However, the determinants were found to be with naked pDNA transfection as 2.64%. The results obtained from the study reveals that newly designed CSLN and OLN non-viral vector systems with high transfection efficiency and low cytotoxicity are good vector systems for the delivery of reprogramming factors. Besides, the expression of OCT-4/SSEA-4 in cells transfected with OLN-pDNA is higher than in cells transfected with CSLN-pDNA. Thus, OLN is more efficient compared to CSLN for the delivery of reprogramming transcription factors.
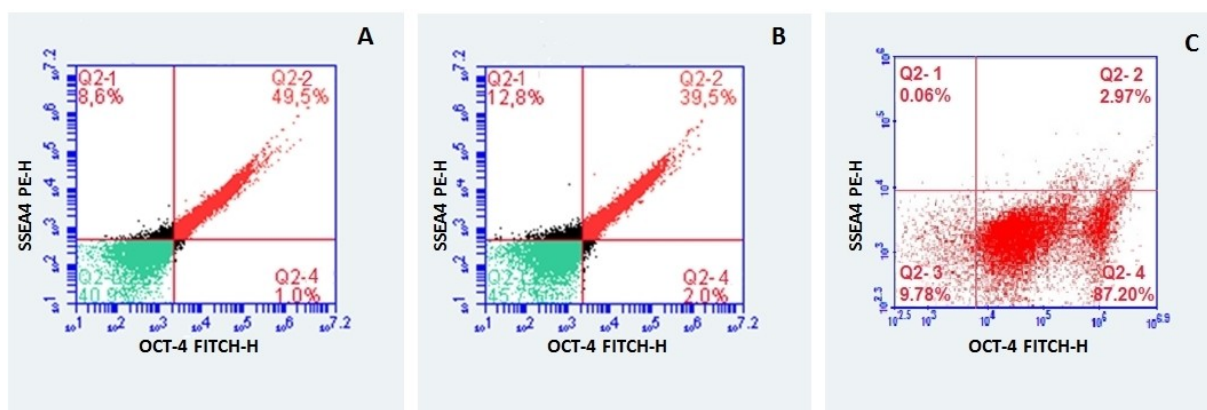

Figure 6. Flow cytometry analysis of cells OLN- pDNA mediated transfection (A), CSLN- pDNA mediated transfection (B) and treated with naked pDNA (C).

ChemistryOpen

Full Papers
doi.org/10.1002/open.202000244

Chemistry
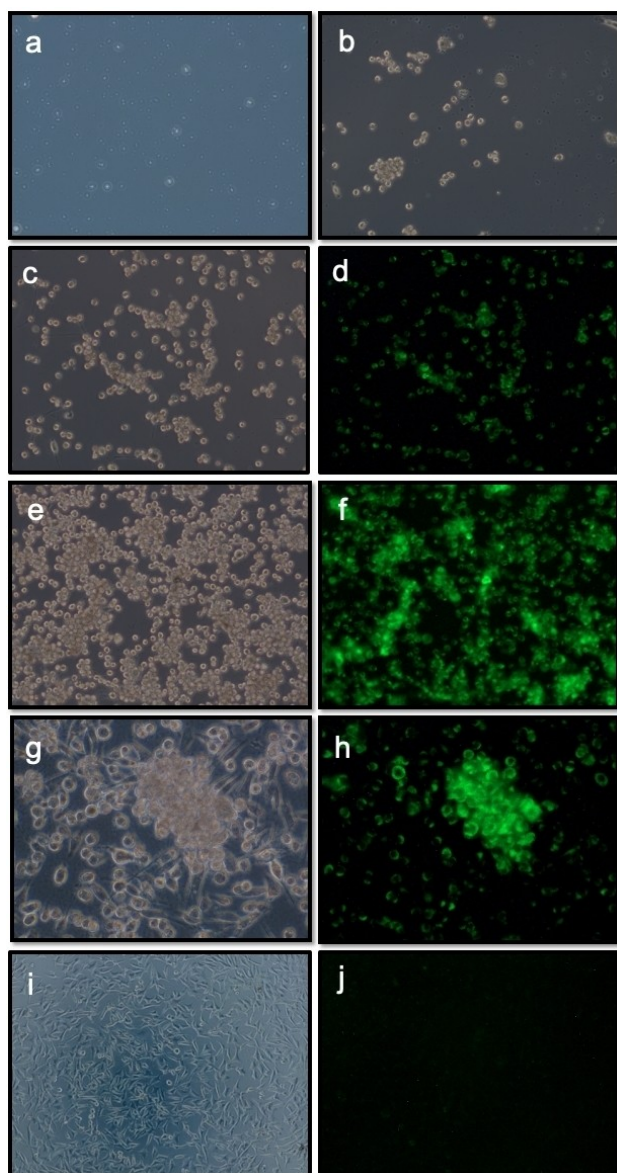Europe
European Chemical
Societies Publishing

Figure 7. Microscopy images of Fibroblast L929 cell line transfected with conjugate III (a) 1st day (10× phase contrast); (b) 6st day (10× phase contrast); (c) 7th day (10× phase contrast); (d) 7th day (10× fluorescence microscopy); (e) 10th day (10× phase contrast); (f) 10th day (10× fluorescence microscopy); (g) 12th day (20x phase contrast); (h) 12th day (20x fluorescence microscopy); Microscopy images of non-transfected Fibroblast L929 cell line; (i) (10× phase contrast); (j) (10× fluorescence microscopy).

Author Contributions

N.T.L. and M.D: conception and design, data analysis and interpretation, final approval of the manuscript; E.K: collection and/or assembly of data, data analysis and interpretation, final approval of the manuscript; F.A. and S.V: collection and/or assembly of data, data analysis and interpretation, manuscript writing, final approval of the manuscript.

Data Availability

The raw/processed data required to reproduce these findings cannot be shared at this time as the data also forms part of an ongoing study.

Conflicts of Interest

The authors declare no conflict of interests.

Keywords: cationic nanoparticle · fibroblast · induced pluripotent stem cell · reprogramming factors · stearamide

[1] K. Takahashi, S. Yamanaka, *Cell* **2006**, *126*, 663–676.
[2] A. Trounson, N. D. DeWitt, *Nat. Rev. Mol. Cell Biol.* **2016**, *17*, 194.
[3] a) N. Nayerossadat, T. Maedeh, P. A. Ali, *Adv. Biomed. Res.* **2012**, *1*; b) M. A. Kotterman, T. W. Chalberg, D. V. Schaffer, *Annu. Rev. Biomed. Eng.* **2015**, *17*, 63–89.
[4] a) C. E. Thomas, A. Ehrhardt, M. A. Kay, *Nat. Rev. Genet.* **2003**, *4*, 346; b) Y. Zhang, A. Satterlee, L. Huang, *Mol. Ther.* **2012**, *20*, 1298–1304.
[5] a) H. S. Loring, M. K. ElMallah, T. R. Flotte, *Hum. Gene Ther: Methods.* **2016**, *27*, 49–58; b) W. S. M. Wold, K. Toth, *Curr. Gene Ther.* **2013**, *13*, 421–433.
[6] G.-W. Jeong, J.-W. Nah, *Carbohydr. Polym.* **2017**, *178*, 322–330.
[7] S. Patil, Y.-G. Gao, X. Lin, Y. Li, K. Dang, Y. Tian, W.-J. Zhang, S.-F. Jiang, A. Qadir, A.-R. Qian, *Int. J. Mol. Sci.* **2019**, *20*, 5491.
[8] a) N. T. Laçin, K. Kızılbey, *Handbook of Nanoparticles*, Springer. (2016) 'Nanoparticles As Non-Viral Transfection Agents'. (ISBN: 9781439898796) Doi:10.1007/978-3-319-15338-4 40. Pp (891–921); b) S.-d. Li, L.-y. Huang, *Gene Ther.* **2000**, *7*, 31.
[9] S. K. Samal, M. Dash, S. Van Vlierberghe, D. L. Kaplan, E. Chiellini, C. Van Blitterswijk, L. Moroni, P. Dubruel, *Chem. Soc. Rev.* **2012**, *41*, 7147–7194.
[10] K. S. Soppimath, T. M. Aminabhavi, A. R. Kulkarni, W. E. Rudzinski, *J. Controlled Release* **2001**, *70*, 1–20.
[11] W. Mehnert, K. Mäder, *Adv. Drug Delivery Rev.* **2012**, *64*, 83–101.
[12] R. H. Müller, D. Rühl, S. Runge, K. Schulze-Forster, W. Mehnert, *Pharm. Res.* **1997**, *14*, 458–462.
[13] S. Doktorovova, R. Shegokar, E. Rakovsky, E. Gonzalez-Mira, C. M. Lopes, A. M. Silva, P. Martins-Lopes, R. Muller, E. B. Souto, *Int. J. Pharm.* **2011**, *420*, 341–349.
[14] A. del Pozo-Rodríguez, D. Delgado, M. Á. Solinís, J. L. Pedraz, E. Echevarría, J. M. Rodríguez, A. R. Gascón, *Int. J. Pharm.* **2010**, *385*, 157–162.

[15] M. L. Bondi', A. Azzolina, E. F. Craparo, N. Lampiasi, G. Capuano, G. Giammona, M. Cervello, *J. Drug Targeting* **2007**, *15*, 295–301.

[16] S. L. Pal, U. Jana, P. K. Manna, G. P. Mohanta, R. Manavalan, *J. Appl. Pharm. Sci.* **2011**, *1*, 228–234.

[17] a) D. Zhou, L. Cutlar, Y. Gao, W. Wang, J. O'Keeffe-Ahern, S. McMahon, B. Duarte, F. Larcher, B. J. Rodriguez, U. Greiser, *Sci. Adv.* **2016**, *2*, e1600102; b) M. Zeng, D. Zhou, F. Alshehri, I. Lara-Sáez, Y. Lyu, J. Creagh-Flynn, Q. Xu, J. Zhang, W. Wang, *Nano Lett.* **2018**, *19*, 381–391; c) S. Liu, Y. Gao, D. Zhou, M. Zeng, F. Alshehri, B. Newland, J. Lyu, J. O'Keeffe-Ahern, U. Greiser, T. Guo, *Nat. Commun.* **2019**, *10*, 1–14.

[18] S. Liu, D. Zhou, J. Yang, H. Zhou, J. Chen, T. Guo, *J. Am. Chem. Soc.* **2017**, *139*, 5102–5109.

[19] M. R. Kumar, U. Bakowsky, C. Lehr, *Biomaterials* **2004**, *25*, 1771–1777.

[20] C. Olbrich, U. Bakowsky, C.-M. Lehr, R. H. Müller, C. Kneuer, *J. Controlled Release* **2001**, *77*, 345–355.

[21] a) J. Ru, X. Qian, Y. Wang, *Cellulose* **2018**, *25*, 5443–5454; b) L. Zhang, H. Yin, Z. Xiong, Y. Xiong, W. Xu, *J. Macromol. Sci., Part B: Phys.* **2011**, *50*, 2255–2270.

[22] H. S. Varli, F. Alkan, M. Demirbilek, N. Türkoğlu, *J. Nanopart. Res.* **2019**, *21*, 237.

[23] E. Y. Kim, K. Jeon, H. Y. Park, Y. J. Han, B. C. Yang, S. B. Park, H. M. Chung, S. P. Park, *Cell. Reprogram.* **2010**, *12*, 627–639.

[24] Y. Piao, S. Hung, S. Lim, R. Wong, M. Ko, *Stem Cells Transl. Med.* **2014**, *3*, 787–791.

[25] N. T. Lacin, K. Kizilbey, B. Mansuroğlu, *Handbook of Nanoparticles*, (**2015**) Muscle Cell and Tissue: Use of Biomaterials and Biomolecules for the Prevention of Restenosis. Intechopen 2015-09-02. DOI: 10.5772/61081.

[26] P. Sundaramoorthy, R. Baskaran, S. K. Mishra, K.-Y. Jeong, S. H. Oh, B. K. Yoo, H. M. Kim, *Colloids Surf. B* **2015**, *135*, 793–801.

[27] A. González-Paredes, L. Sitia, A. Ruyra, C. J. Morris, G. N. Wheeler, M. McArthur, P. Gasco, *Eur. J. Pharm. Biopharm.* **2019**, *134*, 166–177.

[28] K. Tabatt, M. Sameti, C. Olbrich, R. H. Müller, C.-M. Lehr, *Eur. J. Pharm. Biopharm.* **2004**, *57*, 155–162.

[29] H. Lv, S. Zhang, B. Wang, S. Cui, J. Yan, *J. Controlled Release* **2006**, *114*, 100–109.

[30] J. Van Meerloo, G. J. Kaspers, J. Cloos, *Cancer cell culture*, Springer **2011**, pp. 237–245.

[31] a) J. A. Kulkarni, J. L. Myhre, S. Chen, Y. Y. C. Tam, A. Danescu, J. M. Richman, P. R. Cullis, *Nanomedicine* **2017**, *13*, 1377–1387; b) C. Carrillo, N. Sánchez-Hernández, E. García-Montoya, P. Pérez-Lozano, J. M. Suñé-Negre, J. R. Ticó, C. Suñé, M. Miñarro, *Eur. J. Pharm. Sci.* **2013**, *49*, 157–165; c) K. Tabatt, C. Kneuer, M. Sameti, C. Olbrich, R. H. Müller, C.-M. Lehr, U. Bakowsky, *J. Controlled Release* **2004**, *97*, 321–332; d) Y. Han, P. Zhang, Y. Chen, J. Sun, F. Kong, *Int. J. Mol. Med.* **2014**, *34*, 191–196.

[32] S. H. Choi, S.-E. Jin, M.-K. Lee, S.-J. Lim, J.-S. Park, B.-G. Kim, W. S. Ahn, C.-K. Kim, *Eur. J. Pharm. Biopharm.* **2008**, *68*, 545–554.

[33] H. R. Kim, I. K. Kim, K. H. Bae, S. H. Lee, Y. Lee, T. G. Park, *Mol. Pharm.* **2008**, *5*, 622–631.

[34] G. U. Güven, N. T. Laçin, E. Pişkin, *J. Tissue Eng. Regener. Med.* **2008**, *2*, 155–163.

[35] S. Honary, F. Zahir, *Trop. J. Pharm. Res.* **2013**, *12*, 265–273.

[36] E. R. Lee, J. Marshall, C. S. Siegel, C. Jiang, N. S. Yew, M. R. Nichols, J. B. Nietupski, R. J. Ziegler, M. B. Lane, K. X. Wang, *Hum. Gene Ther.* **1996**, *7*, 1701–1717.

[37] Y. H. Yu, E. Kim, D. E. Park, G. Shim, S. Lee, Y. B. Kim, C.-W. Kim, Y.-K. Oh, *Eur. J. Pharm. Biopharm.* **2012**, *80*, 268–273.

[38] X. Qu, T. Liu, K. Song, X. Li, D. Ge, *PLoS One* **2012**, *7*.

[39] M. Khan, K. Narayanan, H. Lu, Y. Choo, C. Du, N. Wiradharma, Y.-Y. Yang, A. C. Wan, *Biomaterials* **2013**, *34*, 5336–5343.